

Post-rift seaward downwarping at passive margins: new insights from southern Oman using stratigraphy to constrain apatite fission-track and (U–Th)/He dating

Yanni Gunnell

Laboratoire de Géographie Physique, Université Paris 7, 2 place Jussieu, 75251 Paris Cedex 5, France

Andy Carter

School of Earth Science, Birkbeck College, University of London, Malet St., London WC1E 7HX, UK

Carole Petit

Marc Fournier

Laboratoire de Tectonique, Université Paris 6, 4 place Jussieu, 75252 Paris Cedex 5, France

ABSTRACT

The plateau edge of southern Oman is used as a natural laboratory to independently test apatite fission-track analysis, (U–Th)/He dating, and stratigraphy as methods for quantifying post-rift erosion depths and lithospheric response at passive margins. A mappable unconformity between the Proterozoic basement and the low-conductivity, pre-rift sediment cover links residual buttes preserved at the coast to the escarpment, and therefore imposes tight constraints on parameter choices for modeling the Cenozoic topographic evolution. A coast-to-scarp denudation depth of ~ 1.75 km and a geothermal gradient of ~ 33 °C·km⁻¹ provide the best fits to the thermochronologic data. With a lithospheric elastic thickness of 7 km, the resulting flexural response generates a retreat and uplift of the escarpment associated with a seaward downwarp of the unconformity, made possible because denudation minima occur inboard of the escarpment and sediment loading occurs offshore. This closed experiment confirms the value of low-temperature thermochronology as a tool for quantifying long-term erosion, but also highlights the distinct advantage of forward modeling over inverse methods in terms of attaining geologic accuracy. This study suggests that post-rift downwarping of eroded rift shoulders can occur, and may have not been commonly

detected because low-temperature thermochronology datasets lack suitable geologic constraints.

Keywords: thermochronology, rifted margin, denudation, flexure, Oman

INTRODUCTION

Low-temperature thermochronology (LTT) is commonly used to detect the depth and timing of erosion at 10–100 Ma time scales at rifted continental margins (e.g., Braun and van der Beek, 2004), but cooling histories are indexed on a thermal reference frame within the Earth's crust. Conversion to a stratigraphic and topographic frame is therefore underpinned by an array of assumptions. In most models of rifted margin evolution, (i) the geometry of initial topography is arbitrary because constraints on initial and boundary conditions are lacking, (ii) the value of pre-rift continental freeboard is speculative, and (iii) estimates of lithospheric elastic thickness (EET) are indexed on the response to erosional unloading of the poorly defined initial topographic parameters. Sensitivity to initial conditions is often tested by letting geometries and EET vary, but solutions will be nonunique.

Depths of erosion, which control the isostatic response of the plateau edge to unloading, are routinely obtained by thermal modeling of apatite fission track (AFT) data, more recently in combination with apatite (U–Th)/He (hereafter AHe) ages. Assumptions made while converting rock cooling rates to denudation rates typically deal with nonunique rock-cooling paths and uncertainties in geothermal gradients. This further affects estimates of the magnitude and timing of denudation, which are critical in determining appropriate isostatic response functions of the lithosphere to unloading. In summary, long-term passive margin evolution models are sensitive to parameter choices, which profoundly affect our understanding of how landscapes evolve (Gunnell et al., 2003).

Optimal solutions can nevertheless be significantly narrowed when constraints afforded by independent data exist. This study focuses on southern Oman, where robust stratigraphic constraints suited to reconstructing long-term topographic evolution are available. Given the parameter-sensitivity of LTT modeling, the objective here was to

assess how well LTT can independently (i) provide matching estimates of the stratigraphically obtained denudation depths, and (ii) reveal the coast-to-scarp pattern of denudation.

METHOD: NON-RADIOMETRIC APPROACH

The southern edge of the Arabian plateau is a nonvolcanic, oblique-rifted margin (Fournier et al., 2004; Bellahsen et al., 2006). The plateau terminates as the south-facing Jabal Samhan escarpment (Fig. 1), rising to elevations of 1.8 km. It consists of a ~1-km-thick sediment package tilted northward by a few degrees and overlying the Proterozoic basement. The age of rifting is not precisely established (see DR¹) but extensional tectonics occurred after 35 Ma (Watchorn et al., 1998) and before the onset of sea-floor spreading in the eastern Gulf of Aden at 18 Ma (Leroy et al., 2004). Continental freeboard afforded by initial shoulder uplift provided the energy for anti-dip streams to drive scarp evolution (Petit et al., in press).

Key stratigraphic constraints on the denudation history of Jabal Samhan are summarized here. (i) The conformable Eocene marine sequence capping the plateau allows calculation of vertical uplift, eroded thicknesses, and fault throws. The pre-rift paleotopography coincided with the top of the youngest Eocene marine deposit, which remains uneroded ~100 km inland from the coastline where it was uplifted to elevations of ~0.6 km a.s.l. and preserved (Fig. 2). (ii) The Afro-Arabian land surface at the K/T boundary was a low-lying erosional plain capped by thin sedimentary Paleozoic and Cretaceous rocks, subsequently inundated and buried below sea level by the Cenozoic marine sequence. The corresponding stratigraphic unconformity is continuously exposed at the escarpment. It can be used to track crustal deformation caused by rifting, erosion, isostasy, and basement burial depths and potential thermochronometric signatures. The coastal plain is entirely cut in basement rocks, which have been eroded to some depth below the basal unconformity due to rift-flank uplift. Critical to this study is the presence of buttes near the coastline, which retain the sedimentary caprock of the escarpment (Figs 1 and 2). Detailed mapping (Platel et al., 1992, Mercolli et al.,

¹ GSA Data Repository item XXX, details on flexural and thermal modeling, LTT analytic procedures, and related figures and data tables are available online at www.geosociety.org/pubs/XXXXX

2006) indicates that their preservation is not afforded by localized downfaulting. Instead, they have survived because of limited erosion occurring at those sites. Because the unconformity can be projected seaward from the escarpment to the buttes (Fig. 2), these provide important geometric data points for reconstructing erosion depths. A numerical model of the Dhofar margin (Petit et al., in press), in which peak denudation depths in the inner coastal belt and sediment loading offshore explain the observed seaward flexural deformation of the margin, has provided EET values of 7 ± 1 km based on simultaneous best fits to the topography and the unconformity.

METHOD: RADIOMETRIC APPROACH

The non-radiometric reconstruction stands alone (Petit et al., in press) but serves here as a reference frame against which to assess the accuracy of radiometrically-derived denudation rates routinely used in passive margin settings (Gallagher et al., 1998). Nine samples (Fig. 1D) were collected across the coastal plain for LTT analysis in order to quantify denudation (see DR for analytic procedure). AFT and AHe partial annealing and retention zones (PAZ and PRZ), respectively, span a range of temperatures with partially overlapping sensitivity windows. Depending on the cooling rate, this approach can reconstruct cooling histories for low chlorine apatites through the temperature range of ~ 120 °C to ~ 40 °C. AFT and AHe ages can be interpreted as cooling ages if cooling is monotonic and fairly rapid because annealing and diffusive losses remain limited. When cooling is slower or locally complicated, only ‘apparent’ AFT and AHe ages can be defined. To understand the significance of such data, modeling packages (e.g. Ketchum, 2005) are used to define probable thermal histories. Because thermal modeling is often used in settings where independent constraints on paleoburial depths are unknown, LTT studies predominantly use random searches of optimal constraints on time–temperature (t–T) histories permitted by the measured AFT and AHe data. Instead, the well constrained stratigraphic setting in Dhofar provides a rare opportunity for implementing forward modeling of the t–T data, a procedure in which thermal histories are fitted empirically to predefined, independent geologic constraints. This approach predicts what combination of measured AFT and AHe parameters would be

expected from a sample that has undergone a predefined t - T history. It also affords indirect constraints on geothermal gradients in regions lacking heat flow data.

RESULTS

All AFT samples (DR Table 1) exhibit mean track lengths (MTL) $< 14 \mu\text{m}$ and a wide scatter in central ages (Fig. 3). None of the ages can therefore be interpreted as straightforward rapid cooling ages, which is typical of most passive margins. AFT ages are much older than the rifting age, which in combination with partially annealed track distributions (Fig. 3) suggests maximum paleoburial temperatures of 70–100 °C maintained over a relatively long period of time. As such, the AFT signatures are typical of an outcropping PAZ. This is confirmed by the survival of short tracks in all the distributions. An extreme case is S9, where the bimodal track distribution and relatively young age suggests a complex thermal history.

Although only three samples (S4, S6, S9) yielded apatite crystals of suitable quality for AHe, these samples span the entire, topographically uniform coastal plain. They all point to rapid cooling after ~ 32 Ma and therefore record the denudational response to rifting. An AHe age does not, however, necessarily refer to a distinct geologic event because a range of t - T paths can yield the same AHe age (Wolf et al., 1998). Samples here are likely to have been long exposed to temperatures corresponding to the ^4He PRZ. In sum, because the sampled basement rocks were situated at < 2 – 3 km depths and hence shallower than the AFT closure isotherm, cooling histories were complex. More robust constraints on cooling histories were therefore searched by combined thermal modeling of AFT and AHe data using the HeFTy program (Ketcham, 2005; see DR) and its multikinetic apatite annealing model. Because AFT annealing kinetics are sensitive to parameter choices, we measured the kinetic parameter D_{par} for each sample (Donelick et al., 1999). D_{par} (in μm) is the mean fission-track etch pit diameter parallel to the c -axis and serves as a proxy for determining chemistry-dependent AFT annealing behavior at crystal level (see DR). Four key requirements guided the forward search for best-fitting t - T paths. These were present-day mean surface temperature (~ 30 °C); an onset of rifting at 25 ± 10 Ma; Eocene paleotemperatures compatible with burial under 0.9 km of sedimentary rocks;

and comparatively shallow depths during the late Cretaceous because Coniacian layers (91–87 Ma) are capped by bauxite (Roger et al., 1989), a surface weathering material. Pre-Cretaceous histories were unknown and therefore left as free parameters.

Despite weak evidence for minor sources of variation due to compositional effects on response to annealing of a few individual apatite grains (see DR and Fig. DR1), all the individually modeled samples exhibit relatively coherent thermal histories (Fig. 3), and hence a common geomorphic past with an onset of rapid cooling at 32–20 Ma. Denudation rates [$\text{km}\cdot\text{Ma}^{-1}$] are routinely estimated from cooling rates [$^{\circ}\text{C}\cdot\text{Ma}^{-1}$] for a given geothermal gradient [$^{\circ}\text{C}\cdot\text{km}^{-1}$]. Here, the key concession to attaining optimal agreement between the stratigraphy-derived (e.g. 1.75 km: cf. Fig. 2) and LTT-derived denudation depths involves a geothermal gradient of $\geq 33\text{ }^{\circ}\text{C}\cdot\text{km}^{-1}$. Such a value for a craton is high, but nevertheless consistent with a cooler cratonic gradient having locally steepened prior to rifting by burial beneath the low-conductivity carbonate package. Blanketing increased the geotherm in the sampled underlying rock units while retaining normal background levels deeper in the crust.

DISCUSSION

Thermal modeling strategies form a continuum between inverse and forward procedures. With inversion schemes, the search for optimal solutions is loosely guided by a broad t – T parameter space, in which large numbers of forward t – T models are generated randomly and ranked by some statistical goodness-of-fit (GOF) criterion. However, GOF does not guarantee the geologic uniqueness (and hence accuracy) of solutions because parameter choices (including the fitness test) determine the outcome as much as the data themselves (Ketcham, 2005). Here, attempts at inverse modeling the data yielded far less robust results, capturing only the late Cenozoic rapid cooling event with inferior precision on timing. With forward modeling, the double unknown of denudation rate and geothermal gradient are reduced to just the latter. This could imply that the success of LTT as a method in quantitative geomorphology is driven by the quality of external inputs and, therefore, falls prey to circular reasoning. However, the internal consistency of this study also indicates that if most required parameters are available, LTT on its own will predict mean denudation values with some accuracy.

Geology strives to reconstruct continuous histories with incomplete archives, and so any source of data likely to narrow the range of uncertainty specific to inverse modeling is extremely valuable.

The capacity of LTT to robustly support or challenge geomorphic models of scarp evolution is affected by its inability to detect spatial differences in relative denudation depths $\leq \sim 1$ km. Here this is apparent in the inability of the data to resolve the coast-to-scarp erosion gradients dictated by the stratigraphy (Fig. 2). Fitting calculated denudation depths to the stratigraphically determined values of Fig. 2 would only be possible if different geothermal gradients were assumed for each sample. This seems implausible across such a small geographic area, and would require unrealistically high values ($> 50 \text{ }^\circ\text{C}\cdot\text{km}^{-1}$) for the less eroded coastal area. Currently, geomorphic models envisage initial scarp geometries either as crustal downwarps, shoulder upwarps, or degrading plateau edges (e.g. Braun and van der Beek, 2004). Downwarps are difficult to detect either in rock packages or in the topography but at volcanic margins, seaward flexural deformations have been interpreted as syn-rift roll-over structures (Sheth, 1998; Lenoir et al., 2003). They can also be generated flexurally (Gunnell and Fleitout, 1998) or supported dynamically (Morley and Westaway, 2006) by the effects of post-rift sediment- and/or cooling-related loads. Applying suitably constrained EET values, the Oman example shows that seaward downwarping can occur and affect a footwall upland (Fig. 2) providing that post-rift erosion and sedimentation are distributed so as to cause maximum flexural uplift in the inner coastal belt. Unlike Ollier and Pain (1997), who advocate topographic warping of the pre-rift plateau surface and thus its preservation at the coast, we suggest that seaward downwarping is not incompatible with rift-shoulder uplift (for instance caused by mechanical unloading of the lithosphere during initial tectonic extension: Petit et al., in press).

However, we conceive it as a post-rift phenomenon in which (i) sediment loading occurs offshore; and (ii) denudation minima occur inboard of the escarpment (here due to aridity) on a regional scale, and locally near the coast where the buttes have been preserved as islands of low erosion between catchments expanding into the interior.

The resulting geometry superficially mimics topographic warping, but unlike the model proposed by Ollier and Pain denudation is emphatically not negligible at the coastline.

CONCLUSION

The occurrence of seaward downwarping at rifted margins has been widely discounted on the basis of denudation signatures derived from LTT inversion schemes. However, absence of evidence is not evidence of absence as AHe and AFT systems often lack the appropriate sensitivity to accurately constrain either post-rift denudation histories or crustal deformation geometries (Braun and van der Beek, 2004; this study).

Furthermore, buttes that would testify to plateau-edge cambering may be rare features with low preservation potential because in non-arid environments they fully erode within 30–40 Ma after rifting. This study emphasizes that LTT is a useful and potentially accurate tool for quantifying long-term denudation rates but that its power to discriminate between theoretical denudation patterns is substantially strengthened by incorporating stratigraphic constraints.

REFERENCES CITED

- Bellahsen, N., Fournier, M., d'Acremont, E., Leroy, S., and Daniel, J.-M., 2006, Fault reactivation and rift localization: The northeastern Gulf of Aden margin: *Tectonics*, v. 25, doi: 10.1029/2004TC001747.
- Braun, J., and van der Beek, P., 2004, Evolution of passive margin escarpments: what can we learn from low-temperature thermochronology?: *Journal of Geophysical Research*, v. 109, F04009, doi: 10.1029/2004JF000147.
- D'Acremont, E., Leroy, S., Beslier, M.-O., Bellahsen, N., Fournier, M., Robin, C., Maia, M., and Gente, P., 2005, Structure and evolution of the eastern Gulf of Aden conjugate margins from seismic reflection data: *Geophysical Journal International*, v. 160, p. 869–890.
- Donelick, R.A., Ketcham, R.A., and Carlson, W.D., 1999, Variability of apatite fission-track annealing kinetics II: Crystallographic orientation effects: *American Mineralogist*, v. 84, p. 1224–1234.

- Fournier, M., Bellahsen, N., Fabbri, O., and Gunnell, Y., 2004, Oblique rifting and segmentation of the NE Gulf of Aden passive margin: *Geochemistry, Geophysics, Geosystems*, 5, Q11005, doi:10.1029/2004GC000731.
- Gallagher, K., Brown, R.W., and Johnson, C.J., 1998, Geological applications of fission track analysis: *Annual Review of Earth and Planetary Sciences*, v. 26, p. 519–572.
- Gunnell, Y., and Fleitout, L. (1998). Shoulder uplift of the Western Ghats passive margin, India — a flexural model: *Earth Surface Processes and Landforms*, v. 23, p. 391–404.
- Gunnell, Y., Gallagher, K., Carter, A., Widdowson, M., and Hurford, A.J., 2003, Denudation history of the continental margin of western peninsular India during the Mesozoic and Cenozoic: *Earth and Planetary Science Letters*, v. 215, p. 187–201.
- Ketcham, R.A., 2005, Forward and inverse modeling of low-temperature thermochronometry data: *Reviews in Mineralogy and Geochemistry*, v. 58, p. 275–314.
- Lenoir, X., Feraud, G., and Geoffroy, L., 2003, High-rate flexure of the East Greenland volcanic margin: constraints from $^{40}\text{Ar}/^{39}\text{Ar}$ dating of basaltic dykes: *Earth and Planetary Science Letters*, v. 673, p. 1–14.
- Leroy, S., Gente, P., Fournier, M., d'Acremont, E., Patriat, P., Beslier, M.-O., Bellahsen, N., Maia, M., Blais, A., Perrot, J., Al-Kathiri, A., Merkouriev, S., Fleury, J.-M., Ruellan, P.-Y., Lepvrier, C., and Huchon, P., 2004, From rifting to spreading in the eastern Gulf of Aden: a geophysical survey of a young oceanic basin from margin to margin: *Terra Nova*, v. 16, p. 185–192.
- Mercolli, I., Briner, A.P., Frei, R., Schönberg, R., Nägler, T.F., Kramers, J., and Peters, T., 2006, Lithostratigraphy and geochronology of the Neoproterozoic crystalline basement of Salalah, Dhofar, Sultanate of Oman: *Precambrian Research*, v. 145, p. 182–206.
- Morley, C.K., and Westaway, R., 2006, Subsidence in the super-deep Pattani and Malay basins of Southeast Asia: a coupled model incorporating lower-crustal flow in response to post-rift sediment loading : *Basin Research*, v. 18, p. 51–84.
- Ollier, C.D., and Pain, C., 1997, Equating the basal unconformity with the palaeoplain: a model for passive margins: *Geomorphology*, v. 19, p. 1–15.

- Petit, C. Fournier, M., Gunnell, Y., in press, Tectonic and climatic controls on rift escarpments: erosion and flexural rebound of the Dhofar passive margin (Gulf of Aden, Oman): *Journal of Geophysical Research (Solid Earth)*.
- Platel, J.-P., Roger, J., Peters, T.J., Mercolli, I., Kramers, J.D., and Le Métour, J., 1992, Geological map of Salalah, Sultanate of Oman, scale 1:250 000, sheet NE 40-09: Oman Ministry of Petroleum and Minerals, Directorate General of Mines.
- Roger, J., Platel, J.-P., Cavelier, C., and Bourdillon-de-Grisac, C., 1989, Données nouvelles sur la stratigraphie et l'histoire géologique du Dhofar (Sultanat d'Oman): *Bulletin de la Société Géologique de France*, v. 2, p. 265–277.
- Sheth, H.C., 1998, A reappraisal of the coastal Panvel flexure, Deccan traps, as a listric-fault-controlled reverse drag structure: *Tectonophysics*, v. 294, p. 143–149.
- Watchorn, F., Nichols, G.J., and Bosence, D.W.J., 1998, Rift-related sedimentation and stratigraphy, southern Yemen (Gulf of Aden), *in* Purser, B.H., Bosence, D.W.J., eds., *Sedimentation and tectonics of rift basins: Red Sea–Gulf of Aden*: Chapman and Hall, London, p. 165–189.
- Wolf, R.A., Farley, K.A., and Kass, D.M., 1998, Modeling of the temperature sensitivity of the apatite (U–Th)/He thermochronometer: *Chemical Geology*, v. 148, p. 105–114.

FIGURE LEGENDS

Fig. 1. Southern Dhofar. A: study area. B: the Jabal Samhan (source: Google Earth). C: topography, bathymetry (from Leroy et al., 2004) and main faults (master fault, MF, after d'Acromont et al., 2005). D: lithology (after Mercolli et al., 2006, simplified) and apatite sample location (S1 to S9). White arrows show buttes.

Fig. 2. Strike-perpendicular cross-section of Jabal Samhan based on Platel et al. (1992).

Fig. 3. Integrated LTT results for southern Dhofar. Best-fitting cooling histories (top left) with track-length distributions (histogram) and their model fits (black curves).

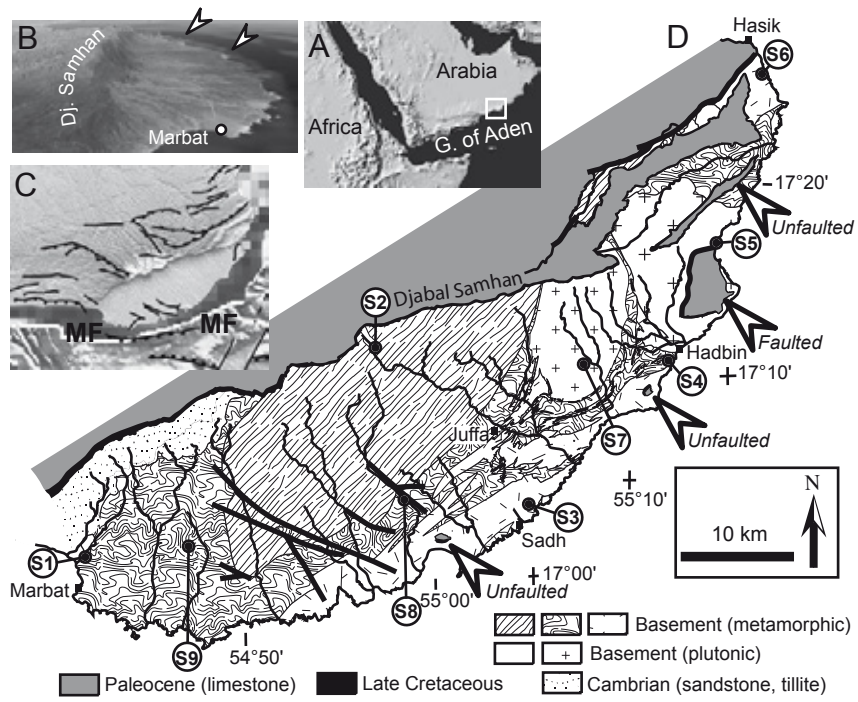
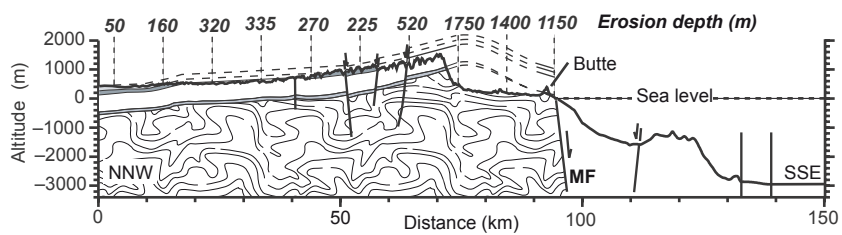


Fig. 1



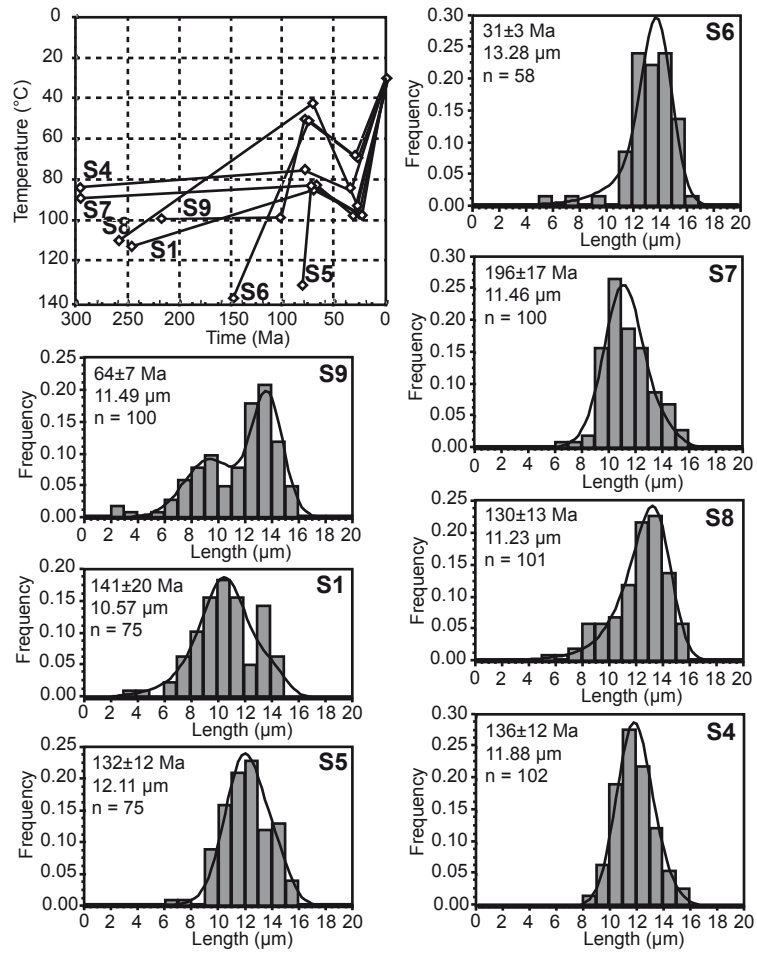


Fig. 3